Malaysian Journal of Analytical Sciences (MJAS)
Published by Malaysian Analytical Sciences Society

ADSORPTION AND MOLECULAR DOCKING STUDY OF BISPHENOL A USING REUSABLE ZIF–8 (ZN) METAL–ORGANIC FRAMEWORKS IN AN AQUEOUS SOLUTION

(Penjerapan dan Kajian Penambatan Molekul Bisfenol A Menggunakan Kerangka Logam–Organik ZIF–8 (Zn) yang boleh Digunakan Semula dalam Larutan Air)

Afzan Mahmad[1, 3], Teh Ubaidah Noh[2], Maizatul Shima Shaharun[3*], Zakariyya Uba Zango[4]

[1]*Laboratory Department,*
Universiti Kuala Lumpur, Royal College of Medicine Perak, Malaysia
[2]*Institute of Bioproduct Development, Universiti Teknologi Malaysia, Malaysia*
[3]*Fundamental and Applied Sciences Department,*
Universiti Teknologi PETRONAS, Seri Iskandar, Perak, Malaysia
[4]*Department of Chemistry, Al-Qalam University, Katsina, Nigeria*

[*]*Corresponding author: maizats@utp.edu.my*

Received: 24 May 2022; Accepted: 18 July 2022; Published: 30 October 2022

Abstract

Bisphenol A (BPA) is a derivative of phenol that has been identified as a pollutant in water. This work aimed to evaluate the experimental and molecular docking findings on the adsorption of BPA using porous material metal–organic frameworks (MOFs) of zeolitic imidazolate frameworks (ZIF–8 (Zn)). The commercial ZIF–8 (Zn) was characterized by field emission scanning electron microscopy (FESEM), scanning electron microscopy (SEM), and energy dispersive X–ray (EDX). The surface morphology of ZIF–8 (Zn) showed cubic particles and zinc components (18.70 %) detected by EDX. The adsorption of endocrine–disruptive chemicals of BPA was performed by batch adsorption experiments and measured using ultraviolet–visible (UV–Vis) spectrophotometry. ZIF–8 (Zn) was shown to achieve adsorption at BPA dosage (0.4 g), and pH 6 (25 ^{o}C) with high BPA removal (98.84%). Molecular docking simulation represented that BPA was bound to ZIF–8 (Zn) via the inner pores. The mechanism interaction of BPA and ZIF–8 (Zn) was via van der Waals interaction. The adsorption of BPA onto ZIF–8 (Zn) fitted the Langmuir isotherm and the pseudo–second–order model. The possible regeneration and reusability of ZIF–8 (Zn) show good suitability for reusable adsorbent in BPA adsorption application from environmental water.

Keywords: bisphenol A, adsorption, ZIF–8, water pollutants, metal–organic frameworks

Abstrak

Bisfenol A (BPA) adalah terbitan fenol yang telah dikenal pasti sebagai bahan pencemar di dalam air. Kerja kajian ini bertujuan untuk menilai ekperimen dan kajian penambatan molekul pada penjerapan BPA menggunakan kerangka kerja logam–organik (MOFs) bahan berliang iaitu kerangka besi zeolitik imidazolat (ZIF–8 (Zn)). ZIF–8 (Zn) secara komersil dicirikan oleh mikroskopi electron imbasan pancaran medan (FESEM), mikroskopi electron elektron imbasan (SEM), dan sinar–X serakan tenaga (EDX). Morfologi permukaan ZIF–8 (Zn) oleh EDX menunjukkan zarah padu partikel kubik dan komponen zink (18.70 %) dikesan oleh

EDX. Penjerapan BPA yang mengganggu bahan kimia endokrin telah dilakukan oleh secara eksperimen penjerapan kelompok dan diukur menggunakan spektrofotometer ultraungu tampak (UV–Vis). ZIF–8 (Zn) yang ditunjukkan mencapai penjerapan pada dos BPA (0.4 g), pH 6 (25 ºC) dengan penyingkiran BPA yang tinggi (98.84%). Simulasi penambatan molekul menunjukkan bahawa BPA terikat kepada ZIF–8 (Zn) melalui liang dalam. Mekanisma BPA dan ZIF–8 (Zn) adalah melalui interaksi van der Waals. Penjerapan BPA ke atas ZIF–8 (Zn) adalah sepadan dengan model Langmuir dan pseudo–tertib–kedua. Kemungkinan penjanaan dan kebolehgunaan semula untuk ZIF–8 (Zn) menunjukkan kesesuaian yang baik untuk bahan penjerap yang boleh diguna semula dalam aplikasi penjerapan BPA daripada air persekitaran.

Kata kunci: bisfenol A, penjerapan, ZIF–8, pencemaran air, kerangka besi logam–organik

Introduction

Toxic organic compound contamination of water has remained an issue for ecosystems. Endocrine–disrupting compounds of bisphenol A (BPA) and bisphenol S (BPS) have been frequently detected in industrial and environmental water [1]. BPA is widely used in the manufacturing of storage containers, such as plastics [1], water supply pipes [2], reusable water bottles [3–5], and food containers [6–7]. A phenolic molecule with two phenol moieties [8], low vapor pressure, moderate water solubility, and low volatility [9] are some of the characteristics of BPA. BPA is a solid at room temperature and very toxic to aquatic life at concentrations of 1,000 to 10,000 mg/L in freshwater [10–11].

Multiple wastewater treatment strategies have been shown to effectively remove BPA from water [8–10]. Adsorption is one of the promising techniques to remove organic and inorganic pollutants from wastewater [8]. The most commonly used adsorbent is activated carbon and multi–walled carbon nanotubes at both laboratory and industrial scales. However, it has several disadvantages, such as problems with hydrophilic substances, the selective performance of the carbon used, high cost, and the need for complexing agents [2]. Thus, an alternative reusable adsorbent has been proposed to treat BPA wastewater so that the discharged water can comply with environmental regulations.

Metal–organic frameworks (MOFs) are suggested as one of the most advanced materials that can effectively remove toxic pollutants from wastewater. MOFs are organic–inorganic hybrid crystalline porous substances with positively charged metal ions next to organic linker molecules [12]. The compounds offer many advantages, such as ultra–porous structure for the surface area [13], high pore volume [14], uniform particle size [15–18], good thermal and chemical stability [19], and the flexibility of geometrical structures to impart different shapes for the frameworks [10]. These advantages of MOFs have the potential for effective BPA adsorption in wastewater. ZIFs, or zeolitic imidazolate frameworks, are a subclass of MOFs that are primarily composed of tetrahedrally coordinated transition metals such as cobalt, zinc, and imidazolate linkers. They are assembled through the process of self–assembly. With the strong and small bonds of the metal ions–imidazolate, ZIFs are associated with great characteristics as universal adsorbents for adsorption of BPA [19].

According to the findings that were published by Peng et al. [20], the elimination of BPA by employing chitosan–modified zeolite (Ch–Z) in the absence and presence of sodium cholate (NaC) was examined. It was discovered that the elimination of BPA by adsorption onto Ch–Z with NaC was over nine times higher than when there was no NaC present in the experiment. The research conducted by Genc et al. [21] utilized surfactant–modified natural zeolite to remove BPA from aqueous solutions. The robust design technique developed was applied in order to maximize the adsorption of BPA, and the maximum adsorption capacity was reported to be 6.90 mg/g. The adsorption of BPA by modified zeolites containing cetyltrimethyl ammonium bromide (CTAB) and cetylpyridinium bromide (CPB) was investigated by Wang et al. [22]. The most effective modified zeolite for the removal of BPA was found to be one that combined 10% CTAB with pre-treated zeolite and was carried out at a temperature of 25℃ for thirty-six hours. Other research found that the ZIF-8@SBA-15 adsorbent, which was made by modifying the ZIF-8 coating layers using the

coordination method, has a maximum adsorption capacity of 123.4 mg/g for 200 mg/L BPA. More than a twofold increase in adsorption capacity was seen with the ZIF-8@SBA-15 adsorbent, and an almost twentyfold increase in adsorption rate constant was observed [23]. Synthetic zeolite with a NaX structural type was modified with cyclodextrin (CD) in the study conducted by Bandura et al. [24] to improve the adsorption of BPA from aqueous solutions. The adsorption of BPA was consistent with a monolayer model, and it suggested the creation of host–guest complexes along with hydrogen bond formation. The highest adsorption capabilities for the removal of BPA were measured at 32.7 mg/g. According to the adsorption behavior of ZIFs, they can function as an effective adsorbent for the removal of BPA from aqueous media.

In this work, ZIF–8 (Zn) was chosen as the adsorbent in this investigation of the BPA removal from an aqueous solution. There has been no previously published work for ZIF–8 (Zn) utilizing ultraviolet–visible (UV–Vis) spectroscopy that studied regeneration and reusability. The reusable ZIF–8 (Zn) may help in the development of a green adsorbent that will offer a high yield whilst having very low operational expenses. The batch adsorption experiments were measured using scanning electron microscopy (SEM), energy–dispersive X–ray spectroscopy (EDX), field emission scanning electron microscopy (FESEM), and UV–Vis spectrophotometer for absorbance measurement. The effects of parameters were studied for effective BPA adsorption. The thermodynamics, kinetics, and isotherm of the process were also determined, and possible mechanisms step and molecular docking for the BPA adsorption were proposed. By considering reusable adsorbent, ZIF–8 (Zn) could reduce the maintenance cost and be environmentally friendly in the removal of BPA.

Materials and Methods

Chemicals Reagents

The chemicals used in this experiment were analytical grade and had no purification before use. BPA analytical standard (> 99% purity), and Basolite Z1200@ZIF–8 (Zn) (99% purity) was obtained from Sigma–Aldrich (USA). Sodium hydroxide (NaOH), and hydrochloric acid (HCl) were obtained from Avantis Laboratory, Malaysia.

Characterization of ZIF–8 (Zn)

The surface morphology of ZIF–8 (Zn) was determined using FESEM–EDX (Zeiss Supra 55 VP, the United Kingdom). Meanwhile, the equipment was operated at 200 kV and the samples were sputtered–coated with Au metal. EDX was conducted to detect the elemental composition of the ZIF–8 (Zn).

Batch adsorption studies

The experiments were carried out using ZIF–8 (Zn) that was added to 200 mL of BPA solutions. Fig. S1 represents typical calibration curves for the BPA solution. The conical flasks were sealed and placed in a shaker and mixed using an orbital shaker (Daihan Scientific, China). The samples were withdrawn at a certain time interval using a syringe and the residual BPA concentration was analyzed spectrophotometrically by observing the absorbance at the maximum wavelength of absorption (276 nm) using a UV–vis spectrophotometer (Shimadzu, UV–1800). The parameters that affect the adsorption, such as the MOF dosage, temperature, and pH were systematically studied using one parameter at a time (OFAT).

The % BPA removal is stated by the formula below [17]:

$$\%R = \frac{C_o - C_e}{C_o} \times 100\% \quad (1)$$

And the BPA quantity adsorbed at a time (q_t) and equilibrium (q_e) is calculated as:

$$q_t = \frac{(C_o - C_t)V}{w} \quad (2)$$

$$q_e = \frac{(C_o - C_e)V}{w} \quad (3)$$

where C_t is the equilibrium concentration of the BPA (mg/L), C_o is the initial BPA concentration (mg/L), V is the volume of the water (L) and w is the mass of BPA (g).

The adsorption isotherms for BPA were obtained via adsorption for 60 minutes, which is sufficient for

equilibrium. The effect of the ZIF–8 (Zn) dosage (0.05–0.4 g) was investigated and maintained at 90 mg/L. For BPA adsorption under a range of pH (2–12), the pH of the BPA solution (90 mg/L) with 0.4 g of ZIF–8 (Zn) was adjusted, before adsorption, by using 0.10 M HCl or 0.10 M NaOH solution. The effect of changing the BPA removal temperature was also investigated at temperatures ranging from 25 to 45 °C. The results obtained from the effect of adsorption temperatures were used to analyse the thermodynamic values using $\Delta G^{\theta} = -RTInK_C$ where ΔG^{θ} (kJ/mol) is the change in Gibbs free energy, R is gas constant, T is the temperature (K) and K_C is a ratio of the amount of BPA adsorbed onto the ZIF–8 (Zn) to the concentration of BPA at equilibrium. The equation explains the extent of the spontaneity of the removal process.

For thermodynamic calculation, the value Kc represents the distribution coefficient, which refers to the ratio of the amount of BPA adsorbed onto the MOFs (C_{ads}) to the concentration of BPA at equilibrium (C_e). Equation 4 can also be rewritten as [17]:

$$InK_C = \frac{\Delta H^{\theta}}{R} - \frac{\Delta S^{\theta}}{RT} \quad (4)$$

where ΔH^{θ} (kJ/mol) is the enthalpy change and ΔS^{θ} ($Jmol^{-1}K^{-1}$) is the entropy change of the adsorption process.

The regeneration and reusability of ZIF–8 (Zn) was also investigated. Using 100 mL of ethanol solution, the ZIF–8 (Zn) was regenerated by discharging the filtrate and washing the leftover particles away. Following that, the MOFs were vacuum dried at 100 ° C for 3 hours. For stability studies, the samples were stored in a desiccator and remained unaltered during the long–term storage.

Molecular docking simulation

The molecular docking study of the 1:1 ratio of BPA with ZIF–8 (Zn) molecules was conducted using AutoDock Tools version 1.5.6. The docking process was studied by the macromolecule (ZIF–8 (Zn)) and ligand (BPA) into the system. After that, the Autogrid tool in the AutoDock program was used to generate a grid box of 120 × 120 × 120 Å cubic with 0.375 Å spacing points. It was installed wider than ZIF–8 (Zn) and attached to the middle of ZIF–8 (Zn) molecules to verify that the box encompassed the whole surface of ZIF–8 (Zn). Cambridge Crystallographic Data Centre (CCDC) and ChemTube3D (University of Liverpool, ChemTube3D) [25] were also used to achieve the crystallographic parameter of one unit cell of ZIF–8 (Zn). BPA's original structure was obtained via the Automated Topology Builder (ATB) service [25], and it was then optimized that use the DFT technique at the B3LYP/631G* level of theory. The BPA compounds were then presented into the cavity of ZIF–8's macromolecular receptor (Zn). To estimate the potential dock framework of BPA with ZIF–8 (Zn) complex and evaluate the binding energy (ΔG_{bind}), the Lamarckian genetic algorithm (LGA) has been used [17].

$$\Delta G_{bind} = \Delta G_{VDW} + \Delta G_{electrostatic} + \Delta G_{H°bond} + \Delta G_{desolv} + \Delta G_{tor} \quad (5)$$

ΔG_{VDW} represents van der Waal energy, $\Delta G_{H°bond}$ represents hydrogen bonding energy, $\Delta G_{electrostatic}$ refers to electrostatic energy, ΔG_{tor} is torsional free energy and ΔG_{desolv} represents desolvation energy.

Results and Discussion

ZIF–8 (Zn) Characterization

The surface morphology of ZIF–8 (Zn) was determined by FESEM analysis, as depicted in Figure 1(a). From the FESEM images, it is observed that the external surfaces of ZIF–8 (Zn) are relatively smooth with fine pores in a cubic structure (yellow arrows). The particle size of ZIF–8 (Zn) was estimated in the range of 219.2 to 572.1 nm which showed a smaller particle size that could contribute to the high surface area. The porosity of ZIF–8 (Zn) was described by the nitrogen (N_2) adsorption–desorption analysis. ZIF–8 (Zn) showed good BET surface area and pore volume, as highlighted in Mahmad et al. [26] studies, which are the characteristics of a highly porous material. It shows the typical nature of porous materials with ZIF–8 (Zn) having a surface area and pore volume of 1299 m^2/g and 0.6 m^3/g,

respectively. ZIF–8 (Zn) showed a high BET surface area due to the flexible amine group pendants [17]. The pore size of the ZIF–8 (Zn) was determined using Barrett–Joyner–Halenda (BJH) analysis as shown in Fig. 1 (d). Also, the surface elemental composition from the EDX analysis of ZIF–8 (Zn) (Figure 1(b)) proved that the surface elemental compositions consisted of carbon (45.55 %), nitrogen (30.34 %), oxygen (5.41 %), and zinc (18.70 %).

In addition, the ZIF–8 (Zn) with good chemical, thermal, and moisture stability was synthesized and characterized. The ZIF–8 (Zn) is described by the cubic–like particles, indicating the good stability of the MOFs as emphasized in the works of literature [17–18]. To further ascertain the stability of the adsorbents for the *in vivo* application, the ZIF–8 (Zn) had aged in a strong acidic condition (pH 1) for a period of one week. However, the SEM analysis has shown no defect in the structural morphology of the ZIF–8 (Zn) as shown by the images in Fig. 1 (c). The detail on the good stability of the ZIF–8 (Zn) is in the same agreement as previously reported by Molavi et al. [27] and Oveisi et al. [28].

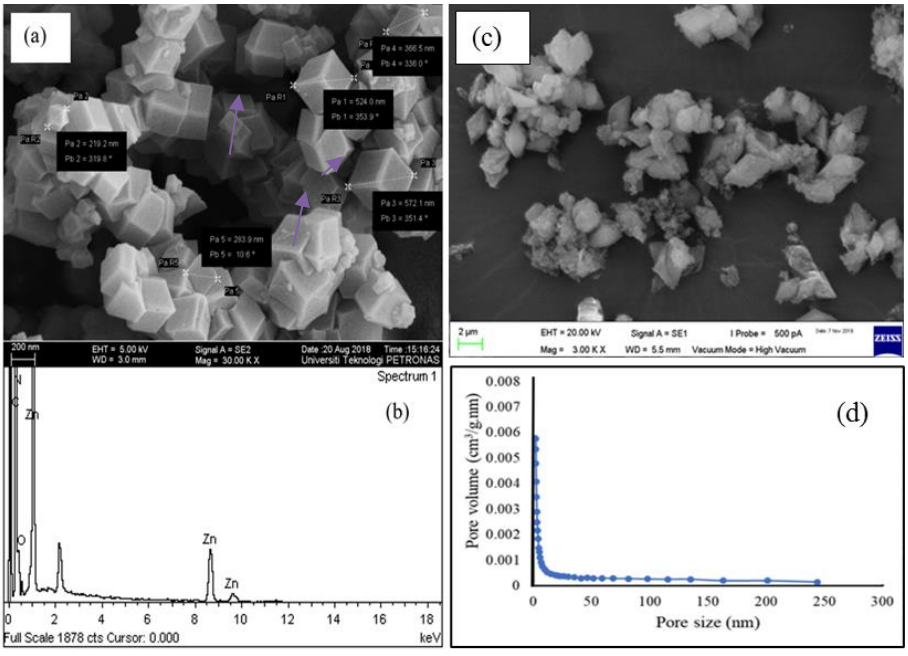

Figure 1. (a) FESEM and (c) SEM images at 30,000× magnification, (b) EDX spectra, and (d) the image of the pore size distribution of ZIF–8 (Zn)

BPA adsorption study

The effect of different dosages of ZIF–8 (Zn) on BPA adsorption was analyzed and the data are shown in Figure 2(a). ZIF–8 (Zn) achieved the highest percentage of BPA removal (98.84 %) at a 0.4 g dosage, which is exactly equivalent to the work done by Zango et al. [17–18]. The mass transfer increased as the dosage of ZIF–8 (Zn) increased, which was determined based on the increase in BPA adsorption capacity. This is because increasing the ZIF–8 (Zn) dosage, increases the number of active pore sites on the surface of ZIF–8 (Zn) for BPA adsorption to occur [29]. At higher dosage, BPA molecules acquired higher equilibrium adsorption capacity due to the increase in the diffusion gradient as the driving force for adsorption [30].

As the pH increased, the removal percentage of BPA decreased (Figure 2 (b)). At the acidic phase, the optimum removal of BPA was 94.68% (pH 6) using ZIF–8 (Zn). Fundamentally, pH affects the electrostatic attraction between ZIF–8 and BPA molecules in an aqueous solution. Based on the results, the adsorption

between ZIF–8 (Zn) and BPA molecules is promoted in an acidic medium. The H^+ ions in the BPA solution are present in an acidic medium, which produced positively charged BPA [17–18]. The BPA removal increased in the presence of acids compared to bases because the negative charge of ZIF–8 (Zn) increases as pH decreases [17]. Hence, there is more electrostatic attraction between ZIF–8 (Zn) and BPA molecules, leading to higher BPA uptake.

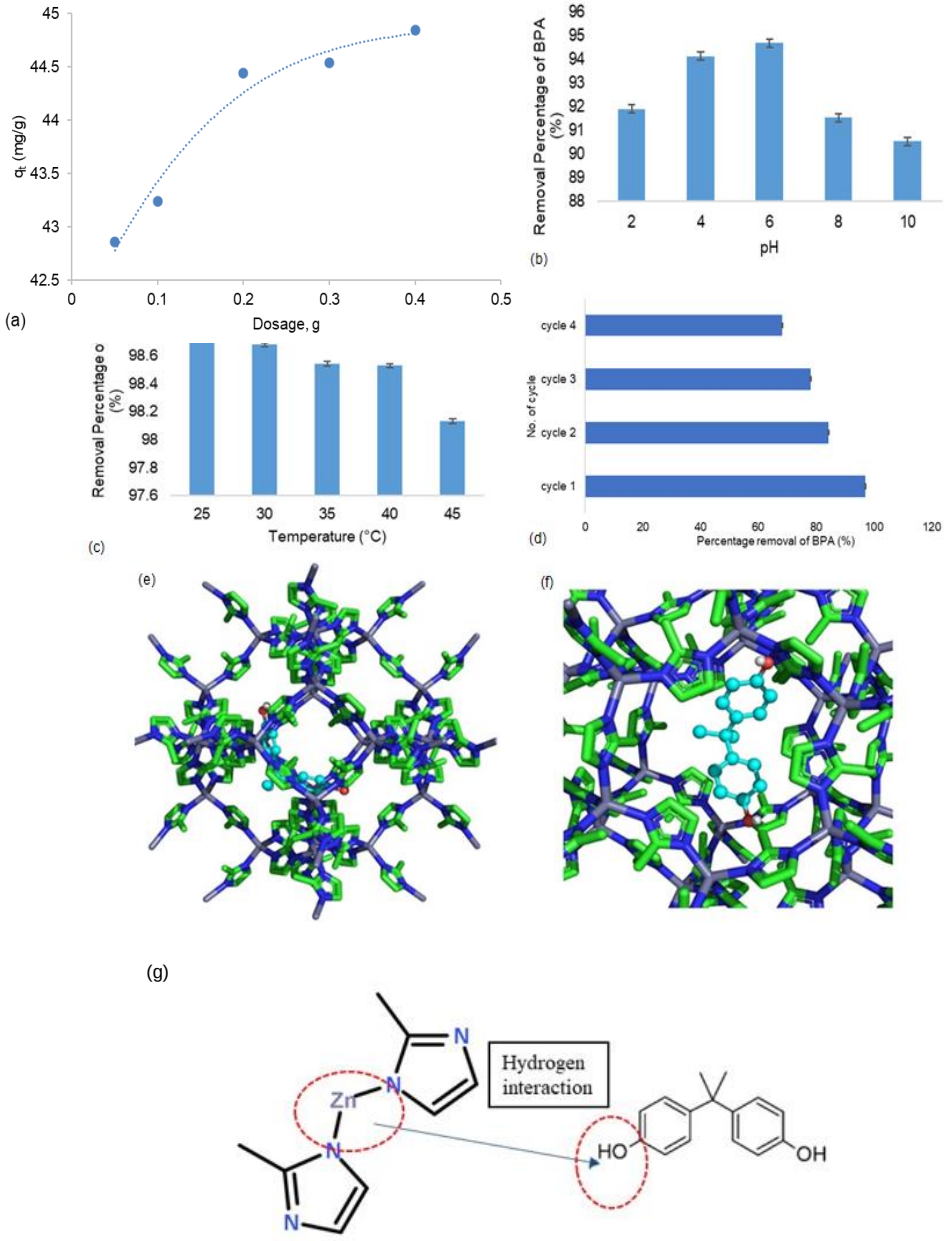

Figure 2. The graph for effect of (a) dosage, (b) pH, (c) temperature, (d) reusability for BPA adsorption onto ZIF–8 (Zn), molecular structure of (e) ZIF–8 (Zn)(BPA) (full view), (f) ZIF–8 (Zn)(BPA) (zoom view) and (g) possible mechanism of ZIF–8 (Zn)(BPA). BPA was colored light blue.

On the other hand, the removal efficiency for ZIF–8 (Zn) at a particular temperature is presented in Figure 1(c). A decrease in the removal percentage of BPA was recorded at accumulated temperatures. As the temperature rises, the mass transfer rate from the bulk solution to the boundary layer near ZIF–8 (Zn) decreases. The increased BPA solubility reveals a lower tendency to the surface of ZIF–8 (Zn) [17–18]. To determine the thermodynamics of the adsorption, Van't Hoff equation was applied and the corresponding enthalpy (ΔH^{θ}), Gibbs free energy (ΔG^{θ}), and entropy changes (ΔS^{θ}) were deduced [17–18] (Table 1). The ΔG^{θ} values were reported to be negative and decreased at high temperatures, indicating a spontaneous and unfavorable nature of the process as the temperature increases [17–18]. The ΔH^{θ} value was 9.957 kJ/mol for ZIF–8 (Zn). This further shows the exothermic and endothermic nature of the BPA adsorption. The rate of diffusion of ZIF–8 (Zn) molecules through the external boundary layers and interior pores of ZIF–8 (Zn) increased as the temperature rises, representing an endothermic adsorption mechanism. The value of ΔS^{θ} was 0.0142 J/mol/K for ZIF–8 (Zn), which showed a high degree of randomness in the ZIF–8 (Zn) adsorption system. In addition, according to Mahmad et al. [26], the adsorption of BPA onto ZIF–8 (Zn) fitted the Langmuir isotherm and the pseudo–second–order model.

Table 1. Thermodynamic parameters for the adsorption of BPA onto ZIF–8 (Zn)

Temp (°C)	ΔG^{θ}(kJ/mol)	ΔH^{θ}(kJ/mol)	ΔS^{θ}(J/mol/K)
25	−14.241		
30	−14.222		
35	−14.424	9.957	0.0142
40	−14.852		
45	−14.632		

After the batch adsorption tests, the regeneration and reusability of ZIF–8 (Zn) demonstrate remarkable potential as adsorbents for BPA removal. The BPA removal percentage obtained by ZIF–8 (Zn) in the 4th cycle was 68.2% (Figure 1 (d)). This finding shows that ZIF–8 (Zn) has good reusability features with good removal performance [17–18]. Zango et al. [17] reported that MOF has the possibility to be regenerated and reused until the 5th cycle with a good percentage of pollutant removal. A significant *p*–value is vital for determining the fit of the model. In other words, a *p*–value < 0.05 indicates the significance of the model for the regression analysis under the influence of independent variables. The temperature and dosage of ZIF–8 (Zn) were considered significant for BPA adsorption. Thus, these values proved that the alternative hypothesis is accepted and there is a difference between the means of the parameters. Meanwhile, the pH of ZIF–8 (Zn) was not statistically significant. This shows that the null hypothesis is accepted and there is no difference between the means of the parameters.

Molecular docking of adsorption of BPA onto ZIF–8 (Zn)

Docking simulation was also performed to analyze the molecular interaction for the BPA removal onto ZIF–8 (Zn). The binding conformers for the complex formation are shown in Figure 1 (e–f) for ZIF–8 (Zn). It was observed that BPA molecules prefer to bind with the internal pores of ZIF–8 (Zn) due to their smaller size [17–18]. The stability of the docking conformers is determined by the binding energy of the inclusion complex formed. It represents the strength and stability of the interaction of ZIF–8 (Zn) with BPA. The result of molecular docking for the interaction of ZIF–8 (Zn) with

BPA was supported by the calculated equilibrium adsorption capacities obtained from the contact time optimization studies with ZIF–8 (Zn) adsorption, where the q_e value was 43.82 ±0.17 mg/g [31]. The BPA adsorption onto ZIF–8 (Zn) exhibited the ΔG_{bind} of −4.21 kcal mol^{-1} [31]. The docking findings follow a pattern that is comparable to that seen in the experimental data collected for the adsorption capacity of ZIF–8 (Zn). More stable physisorption interaction is associated with lower free energy values [32], as opposed to higher free energy values. ZIF–8 (Zn) models were established with BPA and also exhibit van der Waals interactions with the adsorbing contaminants. Table 2 lists the van der Waals as well as electrostatic energies associated with the inclusion complexes, as well as the values of interaction energies. The distance of the hydrogen bond was reported as 3.6 Å. However, the hydrogen bond of ZIF–8 (Zn) was insignificant due to the large average distance (more than 3 Å) from the experimentally determined geometry, which can be due to wrong orientation or displacement (Figure 2 (g)) [32–33]. Hence, due to the lowest ΔG_{bind}, ZIF–8 (Zn) was predicted to have van der Waals interaction with BPA in adsorption studies. Thus, the information obtained from the docking simulation is relevant.

Table 2. The interaction energy of ZIF–8 (Zn) with BPA inclusion complex obtained from molecular docking simulation

Interaction Energy (kcal/mol)					
$\Delta G_{binding}$	$\Delta G_{\text{vdw + HBond + desolv}}$	ΔG_{elec}	ΔG_{total}	$\Delta G_{unbound}$	ΔG_{tor}
−4.21	−5.38	−0.02	−0.50	−0.50	+1.19

Comparison with other adsorbents

Table 3 shows the key features of adsorbents for the removal of BPA from wastewater that have been reported. Based on the reported studies, it is clear that ZIF–8 (Zn) has a higher BPA removal percentage (% R = 98.84 %). The optimum contact time was also rapid (30 minutes) [26], and the ZIF–8 (Zn) was reported with good reusability and regeneration. In contrast to the adsorbents given in Table 3, the listed adsorbents have not undergone any studies on their potential to be regenerated and reused. Because ZIF–8 (Zn) has the capacity to regenerate itself and is reusable, it has the potential to reduce costs, has a high level of efficiency, and is kind to the environment. Despite this, when compared to the other adsorbents, the ZIF–8 (Zn) demonstrated the shortest amount of time necessary for the adsorption of BPA to attain the optimal result. When compared to the other adsorbents, the surface area of ZIF–8 (Zn) was reported as having the greatest value; as a result, ZIF–8 (Zn) has a high potential for future research into the maximum adsorption capacity based on the impact of a high concentration of BPA. As a result of these findings, ZIF–8 (Zn) has the possibility to be a future alternative reusable adsorbent for the removal of BPA.

Table 3. Comparison of reported adsorbents with MOFs used for BPA removal

Adsorbents	Surface Area (m^2/g)	Maximum Adsorption Capacity (mg/g)	Initial Concentration, Solid/Liquid Ratio	Isotherm Models	Kinetic Models	Removal of BPA (%R)	Equilibrium Time	References
Commercial powdered activated carbon	1027	307.00	5–70 mg/L, 10 mg/100 mL	Langmuir	Ps2	>99.00	>90 min	[34]
Palygorskite–montmorillonite	1777	77.30	0.01–10 mg/L, 3 g/25 mL	Langmuir	–	–	>48 hours	[35]
CTAB–modified zeolite	–	37.85	0–200 mg/L, 1 g/L	Freundlich	Ps2	–	–	[22]
Chitosan–modified zeolite (Ch–Z) in the absence and presence of sodium cholate (NaC)	–	77.82	100 µmol/L, 1 g/L, 1.68 mmol/L	Freundlich	Ps2	78.00	<9–10 hours	[20]
Surfactant–modified natural zeolite	–	6.90	10–100 mg/L, 0.25 g/50 mL	Temkin	Ps2	–	30 min	[21]
ZIF–8@SBA–15	722	123.40	200 mg/L	–	Ps2	–	2 min	[23]
Zeolite from fly ash modified with β–cyclodextrin	166	32.70	0.5 g/L	Langmuir	Ps2	–	90 min	[24]
This work ZIF–8 (Zn)	1299	43.81 ± 0.17	90 mg/L, 0.4 g	Langmuir	Ps2	98.84	30 min	[26]

* Ps2=pseudo–second order

Conclusion

The BPA removal onto the commercial ZIF–8 (Zn) has been studied. The high BPA removal percentage was successfully achieved with ZIF–8 (Zn). For the regeneration and reusability studies of ZIF–8 (Zn) for BPA adsorption, the removal percentage achieved 68.2% in the 4th cycle. The van der Waals interaction could occur in the adsorption of BPA, as determined using molecular docking simulation. The Langmuir isotherm and the pseudo–second order model were also compatible with the findings. Molecular docking simulation predicted better interaction between ZIF–8 (Zn) and BPA molecules, which agreed well with the experimental findings. Based on the comparison of previously used adsorbents, ZIF–8 (Zn) was shown to be superior in terms of rapid equilibration (30 min), highest BPA removal, and reusable features. Thus, ZIF–8 (Zn) as a future reusable adsorbent can achieve good results in the removal of BPA from wastewater.

Acknowledgment

This work was sponsored by a grant provided through the Financial Aid from Universiti Teknologi PETRONAS (UTP) and the Ministry of Higher Education Malaysia, FRGS No: FRGS/1/2011/SG/UTP/02/13. The authors acknowledge the use of the facilities within the UTP Centralized Analytical Laboratory (CAL).

References

1. Bhatnagar, A. and Anastopoulos, I. (2017). Adsorptive removal of bisphenol A (BPA) from aqueous solution: a review. *Chemosphere*, 168: 885-902.
2. Min Park, J. and Hwa Jhung, S. (2020). A remarkable adsorbent for removal of bisphenol S from water: aminated metal–organic framework, MIL–101–NH_2. *Chemical Engineering Journal*, 2020:125224.

3. Ohore, O. E. and Songhe, Z. (2019). Endocrine disrupting effects of bisphenol A exposure and recent advances on its removal by water treatment systems. A review. *Scientific African*, 5: e00135.
4. Goldinger, D. M., Demierre, A. L., Zoller, O., Rupp, H., Reinhard, H. and Magnin, R. (2015). Endocrine activity of alternatives to BPA found in thermal paper in Switzerland. *Regulatory Toxicology and Pharmacology*, 71: 453-462.
5. Banaderakhshan, R., Kemp, P., Breul, L., Steinbichl, P., Hartmann, C. and Fürhacker, M. (2022). Bisphenol A and its alternatives in Austrian thermal paper receipts, and the migration from reusable plastic drinking bottles into water and artificial saliva using UHPLC–MS/MS. *Chemosphere*, 286: 131842.
6. Ginter–Kramarczyk, D., Zembrzuska, J., Kruszelnicka, I., Zając–Woźnialis, A. and Ciślak, M. (2020). Influence of temperature on the quantity of bisphenol A in bottled drinking water. *International Journal of Environmental Research and Public Health*. 19(9): 5710.
7. Ali, M., Jaghbir, M., Salam, M., Al–Kadamany, G., Damsees, R. and Al–Rawashdeh, N. (2018). Testing baby bottles for the presence of residual and migrated bisphenol A. *Environmental Monitoring & Assessment*, 191(1): 1-7.
8. Abraham, A. and Chakraborty, P. (2020) A review on sources and health impacts of bisphenol A. *Reviews on Environmental Health*, 35(2): 201-210.
9. Han, C. and Hong, Y. C. (2016). Bisphenol A, hypertension, and cardiovascular diseases: epidemiological, laboratory, and clinical trial evidence. *Current hypertension reports*, 18:1-11.
10. Singh, N. (2016). Exposure to bisphenol–A through excess use of polymer, with environmental toxicity. *International Journal of Scientific Research in Science, Engineering, and Technology*, 2: 454-457.
11 Adamakis, I. S., Malea, P. and Panteris, E. (2018). The effects of bisphenol A on the seagrass *Cymodocea nodosa*: Leaf elongation impairment and cytoskeleton disturbance. *Ecotoxicology and Environmental Safety*,157: 431-440.
12. Pettamanna, A., Raghav, D. and Nair, R. H. (2020). Hepatic toxicity in *Etroplus suratensis* (Bloch 1790): An economically important edible fish in Vembanad fresh water Lake, Kerala, India. *Bulletin of Environmental Contamination and Toxicology*, 105(4): 565-571.
13. Samanidou, V. F. and Deliyanni, E. A. (2020). Metal organic frameworks: Synthesis and application. *Molecules*, 25(4): 960.
14. Tibbetts, I. and Kostakis, G. E. (2020). Recent bio–advances in metal–organic frameworks. *Molecules*, 25(6): 1291.
15. Wang, L. C., Ni, X. J., Cao, Y. H. and Cao, G. Q. (2018). Adsorption behavior of bisphenol A on CTAB–modified graphite. *Applied Surface Science*, 428: 165-170.
16. Hoseinpour, V. and Shariatinia, Z. (2021). Applications of zeolitic imidazolate framework-8 (ZIF-8) in bone tissue engineering: A review. *Tissue and Cell*, 72: 101588.
17. Zango, Z. U., Sambudi, N. S., Jumbri, K., Ramli, A., Hanif Abu Bakar N. H., Saad B., Rozaini, M. N. H., Isiyaka, H. A., Osman, A. M., and Sulieman, A. (2020). An overview and evaluation of highly porous adsorbent materials for polycyclic aromatic hydrocarbons and phenols removal from wastewater. *Water*, 2020: 1-40.
18. Zango, Z. U., Sambudi, N. S., Jumbri, K., Ramli, A., Hanif Abu Bakar, N. H., Saad, B., Rozaini, M. N. H., Isiyaka, H. A., Osman, A. M. and Sulieman, A. (2020). A critical review on metal–organic frameworks and their composites as advanced materials for adsorption and photocatalytic degradation of emerging organic pollutants from wastewater. *Polymers,* 12: 264.
19. Ighalo, J. O., Rangabhashiyam, S., Adeyanju, C. A., Ogunniyi, S., Adeniyi, A. G. and Igwegbe, C. A. (2022). Zeolitic Imidazolate Frameworks (ZIFs) for aqueous phase adsorption – A review. *Journal of Industrial and Engineering Chemistry*, 105: 34-48.
20. Peng, S., Hao, K., Han, F., Tang, Z., Niu, B., Zhang, X. and Hong, S. (2015). Enhanced removal of bisphenol–AF onto chitosan–modified zeolite by sodium cholate in aqueous solutions. *Carbohydrate Polymers*, 130: 364-371.

21. Genç, N., Kılıçoğlu, Ö. and Narci, A. O. (2016). Removal of bisphenol A aqueous solution using surfactant–modified natural zeolite: Taguchi's experimental design, adsorption kinetic, equilibrium, and thermodynamic study. *Environmental Technology*, 38(4): 424-432.
22. Wang, H., Gao, J., Liu, W., Zhang, M. and Guo, M. (2016). Recovery of metal–doped zinc ferrite from zinc–containing electric arc furnace dust: Process development and examination of elemental migration. *Hydrometallurgy*, 166: 1-8.
23. Peng, J., Li, Y., Sun, X., Huang, C., Jin, J., Wang, J. and Chen, J. (2019). controlled manipulation of metal–organic framework layers to nanometer precision inside large mesochannels of ordered mesoporous silica for enhanced removal of bisphenol A from water. *ACS Applied Materials & Interfaces*, 11(4): 4328-4337.
24. Bandura, L., Białoszewska, M., Malinowski, S. and Franus, W. (2021). Adsorptive performance of fly ash–derived zeolite modified by β–cyclodextrin for ibuprofen, bisphenol A and caffeine removal from aqueous solutions–equilibrium and kinetic study. *Applied Surface Science*, 56: 150160.
25. Mahmad A., Shaharun M., Noh T. U., Zango Z. U. and Faisal M. (2022). Experimental and molecular modelling approach for rapid adsorption of bisphenol A using Zr and Fe–based metal–organic frameworks. *Inorganic Chemistry Communication*. 142(2022): 109604.
26. Mahmad, A., Shaharun, M. S., Zango, Z. U., Noh, T. U. and Saad, B. (2021). Adsorptive removal of bisphenol a using zeolitic imidazolate framework (ZIF–8). In: Abdul Karim, S. A., Abd Shukur, M. F., Fai Kait, C., Soleimani, H., Sakidin, H. (eds) *Proceedings of the 6th International Conference on Fundamental and Applied Sciences.* Springer Proceedings in Complexity. Springer, Singapore.
27. Molavi, H., Hakimian, A., Shojaei, A. and Raeiszadeh, M. (2018). Selective dye adsorption by highly water stable metal–organic framework: long term stability analysis in aqueous media. *Applied Surface Science*, 445: 424–436.
28. Oveisi, M., Mahmoodi, N. M. and Asli, M. A. (2019). Facile and green synthesis of metal–organic framework/inorganic nanofiber using electrospinning for recyclable visible–light photocatalysis. *Journal of Cleaner Production,* 222: 669-684.
29. Yu, L., Cheng, J., Yang, H., Lv, J., Wang, P., Li, J. R. and Su, X. (2021). Simultaneous adsorption and determination of bisphenol compounds in water medium with a Zr(IV)–based metal–organic framework. *Microchimica Acta*, 188(3): 83.
30. Zango, Z. U., Sambudi N. S., Jumbri, K., Abu Bakar, N. H., Abdullah, N. A. F., Negim, E. S. M. and Saad, B. (2020). Experimental and molecular docking model studies for the adsorption of polycyclic aromatic hydrocarbons onto UiO−66 (Zr) and NH_2−UiO−66 (Zr) metal−organic frameworks. *Chemical Engineering Science*, 220: 115608.
31. Groom, C. R., Bruno, I. J., Lightfoot, M. P. and Ward, S. C. (2016). The Cambridge structural database. *Acta Crystallographica Section* B, 72: 171-179.
32. Zango, Z. U., Bakar, N. H. H. A., Sambudi, N. S., Jumbri, K., Abdullah, N. A. F., Kadir, E. A. and Saad, B. (2020). Adsorption of chrysene in aqueous solution onto MIL-88 (Fe) and NH2-MIL-88 (Fe) metal-organic frameworks: Kinetics, isotherms, thermodynamics and docking simulation studies. *Journal of Environmental Chemical Engineering*, 8(2): 103544.
33. Xiang, Y., Yan, H., Zheng, B., Faheem, A., Chen, W. and Hu, Y. (2021). *E. coli@* UiO−67 composites as a recyclable adsorbent for bisphenol A removal. *Chemosphere*, 270: 128672.
34. Libbrecht, W., Vandaele, K., De Buysser, K., Verberckmoes, A., Thybaut, J., Poelman, H., Van Der Voort, P. (2015). Tuning the pore geometry of ordered mesoporous carbons for enhanced adsorption of bisphenol A. *Materials,* 8(4): 1652-1665.
35. Berhane, T. M., Levy, J., Krekeler, M. P. S., and Danielson, N. D. (2016). Adsorption of bisphenol A and ciprofloxacin by palygorskite–montmorillonite: Effect of granule size, solution chemistry, and temperature. *Applied Clay Science*, 132-133: 518-527.